

# Reactions of Ground-State $\text{Ti}^+$ and $\text{V}^+$ with Propane: Factors That Govern C–H and C–C Bond Cleavage Product Branching Ratios

Petra A. M. van Koppen,<sup>\*,†</sup> Michael T. Bowers,<sup>†</sup> Chris L. Haynes,<sup>‡</sup> and P. B. Armentrout<sup>\*,‡</sup>

Contribution from the Department of Chemistry, University of California, Santa Barbara, California 93106, and Department of Chemistry, University of Utah, Salt Lake City, Utah 84112

Received December 29, 1997

**Abstract:** Reactions of  $\text{Ti}^+$  and  $\text{V}^+$  with  $\text{C}_3\text{H}_8$ ,  $\text{CH}_3\text{CD}_2\text{CH}_3$ ,  $\text{CD}_3\text{CH}_2\text{CD}_3$ , and  $\text{C}_3\text{D}_8$  are studied to characterize the rate-limiting transition states and determine the factors that control the branching between  $\text{H}_2$  and  $\text{CH}_4$  elimination. For ground-state  $\text{Ti}^+$  reacting with propane, dehydrogenation and demethanation both occur at thermal energy with reaction efficiencies of 17% and less than 1%, respectively. For ground-state  $\text{V}^+$ , dehydrogenation occurs at thermal energy with an efficiency of less than 1% whereas demethanation occurs with a  $0.70 \pm 0.06$  eV threshold. Deuterium-labeling studies indicate that  $\beta$ -H(D) transfer to form the metal ethene dihydride complex or a multicenter elimination of  $\text{H}_2$  is the rate-limiting step for dehydrogenation, while reductive elimination of methane is shown to be rate limiting for demethanation. The product kinetic energy release distributions (KERDs) for  $\text{H}_2$  loss from  $\text{Ti}^+(\text{C}_3\text{H}_8)$  and  $\text{V}^+(\text{C}_3\text{H}_8)$  are both statistical. Modeling the experimental KERDs using statistical phase space theory yields  $D_0^\circ(\text{Ti}^+-\text{C}_3\text{H}_6) = 34.5 \pm 3$  kcal/mol and  $D_0^\circ(\text{V}^+-\text{C}_3\text{H}_6) = 30.7 \pm 2$  kcal/mol. To explain differences in the reactivity of  $\text{Ti}^+$  and  $\text{V}^+$ , the potential energy surfaces of the reactions are discussed in some detail with an emphasis on the importance of spin-orbit-coupled crossings between surfaces of different spin.

## Introduction

Studies of first-row transition-metal ions reacting with simple alkanes in the gas phase have given insight into the mechanism and energetics of C–H and C–C bond activation.<sup>1–13</sup> In our studies of  $\text{Fe}^+$ ,  $\text{Co}^+$ , and  $\text{Ni}^+$  reacting with propane and

deuterated propanes, the results were shown to be consistent with a rate-limiting step associated with initial C–H(D) bond activation for both  $\text{H}_2$  and  $\text{CH}_4$  elimination.<sup>2,3</sup> Recent experimental<sup>14</sup> and theoretical<sup>15</sup> work suggests that late multicenter transition states can also play an important role in these reactions and may in fact be rate limiting. In either case, these studies have concentrated on learning about the rate-limiting step in the reaction, but little could be ascertained about the factors that govern the branching ratios between  $\text{H}_2$  and  $\text{CH}_4$  loss.

Reactions of early metal ions, including  $\text{Ti}^+$  and  $\text{V}^+$ , with propane are substantially less exothermic and give dramatically different branching ratios than those of the late metal ions. They are therefore good candidates for probing the portion of the potential energy surface where the branching ratios are determined. In the high-pressure environment of a flow tube, Tonkyn et al.<sup>12</sup> found that  $\text{V}^+$  primarily forms the  $\text{M}^+$ –propane adduct. The only bimolecular reaction observed at thermal energy was a small (6%) elimination of  $\text{H}_2$ , even though  $\text{CH}_4$  elimination is the more exoergic channel. By comparison, Tonkyn et al. found that  $\text{Ti}^+$  is more reactive, with  $\text{H}_2$  elimination the primary reaction channel and the  $\text{Ti}^+$ –propane adduct and  $\text{CH}_4$  elimination channels are observed to be relatively small (16% and <1%, respectively).<sup>12</sup> Similar results were also obtained by MacTaylor et al.,<sup>16</sup> also in a high-pressure, flow tube environment. Under

<sup>†</sup> University of California.

<sup>‡</sup> University of Utah.

(1) van Koppen, P. A. M.; Kemper, P. R.; Bowers, M. T. In *Organometallic Ion Chemistry*, Freiser, B. S., Ed.; Kluwer Academic Publishers: Dordrecht, The Netherlands, 1996; p 157.

(2) (a) Armentrout, P. B. In *Gas-Phase Inorganic Chemistry*; Russel, D., Ed.; Plenum: New York, 1989; p 1. (b) Armentrout, P. B. *Science* **1991**, *251*, 175. (c) Armentrout, P. B. In *Selective Hydrocarbon Activation: Principles and Progress*, Davies, J. A., Watson, P. L., Liebman, J. F., Greenberg, A., Eds.; VCH: New York, 1990; p 467.

(3) (a) Weisshaar, J. C. In *Advances in Chemical Physics*; Ng, C., Ed.; Wiley-Interscience: New York, 1992; Vol. 82, pp 213–261. (b) Weisshaar, J. C. *Acc. Chem. Res.* **1993**, *26*, 213.

(4) (a) van Koppen, P. A. M.; Brodbelt-Lustig, J.; Bowers, M. T.; Dearden, D. V.; Beauchamp, J. L.; Fisher, E. R.; Armentrout, P. B. *J. Am. Chem. Soc.* **1991**, *113*, 2359. (b) van Koppen, P. A. M.; Brodbelt-Lustig, J.; Bowers, M. T.; Dearden, D. V.; Beauchamp, J. L.; Fisher, E. R.; Armentrout, P. B. *J. Am. Chem. Soc.* **1990**, *112*, 5663. (c) Gidden, J.; van Koppen, P. A. M.; Bowers, M. T. *J. Am. Chem. Soc.*, **1997**, *119*, 3935.

(5) (a) van Koppen, P. A. M.; Kemper, P. R.; Bushnell, J. E.; Bowers, M. T. *J. Am. Chem. Soc.* **1994**, *116*, 3780. (b) van Koppen, P. A. M.; Bowers, M. T.; Fisher, E. R.; Armentrout, P. B. *J. Am. Chem. Soc.* **1994**, *116*, 3780.

(6) Tolbert, M. A.; Beauchamp, J. L. *J. Am. Chem. Soc.* **1986**, *108*, 7509.

(7) Aristov N.; Armentrout, P. B. *J. Am. Chem. Soc.* **1986**, *108*, 1806.

(8) Sanders, L.; Hanton, S. D.; Weisshaar, J. C. *J. Chem. Phys.* **1990**, *92*, 3498.

(9) (a) van Koppen, P. A. M.; Kemper, P. R.; Bowers, M. T. *J. Am. Chem. Soc.* **1992**, *114*, 10941. (b) van Koppen, P. A. M.; Kemper, P. R.; Bowers, M. T. *J. Am. Chem. Soc.* **1992**, *114*, 1083.

(10) (a) Sunderlin, L. S.; Armentrout, P. B. *Int. J. Mass Spectrom. Ion Processes* **1989**, *94*, 149. (b) Aristov, N. Ph.D. Thesis, University California, Berkeley, 1986. (c) Sunderlin, L. S.; Armentrout, P. B. *J. Phys. Chem.* **1988**, *92*, 1209.

(11) Armentrout, P. B.; Beauchamp, J. L. *J. Am. Chem. Soc.* **1981**, *103*, 784.

(12) Tonkyn, R.; Ronan, M.; Weisshaar, J. C. *J. Phys. Chem.* **1988**, *92*, 92.

(13) (a) Jacobson, D. B.; Freiser, B. S. *J. Am. Chem. Soc.* **1983**, *105*, 5197. (b) Jackson, T. C.; Carlin, T. J.; Freiser, B. S. *J. Am. Chem. Soc.* **1986**, *108*, 1120.

(14) Haynes, C. L.; Fisher, E. R.; Armentrout, P. B. *J. Phys. Chem.* **1996**, *100*, 18300.

(15) Holthausen, M. C.; Koch, W. *Helv. Chim. Acta* **1996**, *79*, 1939.

low-pressure, single-collision reaction conditions, Sunderlin et al.<sup>10a</sup> found that  $Ti^+$  reacts with propane primarily by  $H_2$  elimination with small amounts of  $CH_4$  elimination and even smaller  $2H_2$  and  $H_2 + CH_4$  elimination channels observed at thermal energies. Aristov<sup>10b</sup> finds similar behavior for reactions of  $V^+$  and propane with  $H_2$  elimination exceeding  $CH_4$  elimination by over 2 orders of magnitude at thermal energies.

State-selected studies of  $V^+$  and  $C_3H_8$  by Sanders et al.<sup>8</sup> have shown that the  $^3F$ ,  $3d^34s$  excited state of  $V^+$  reacts with propane to eliminate  $H_2$  a factor of 80 times faster than the  $^5D$ ,  $3d^4$  ground state of  $V^+$ . The excited state also eliminates  $CH_4$ , but this channel comprises less than 1% of the total products formed. It is understandable that the excited  $^3F$  state of  $V^+$  reacts more efficiently with propane to eliminate  $H_2$  than the  $^5D$  ground state of  $V^+$  because it is the correct spin to form the  $H-V^+-C_3H_7$  inserted intermediate and because the  $^3F$  state of  $V^+$  has more energy available for reaction. However, an explanation of why  $CH_4$  elimination is so inefficient for the  $^3F$  state is not so obvious. Nor is the rate-limiting step in these reactions, how the branching ratios are determined for both ground- and excited-state  $V^+$  reacting with propane, and why ground-state  $Ti^+$  eliminates both  $H_2$  and  $CH_4$  but primarily  $H_2$  at thermal energy.

To address these questions, we have measured the absolute cross-sections for  $H_2$  and  $CH_4$  loss for both  $Ti^+$  and  $V^+$  reacting with propane as a function of kinetic energy. Labeling studies using the selectively deuterated species  $CH_3CD_2CH_3$ ,  $CD_3CH_2CD_3$ , and  $C_3D_8$  were performed to gain insight into the rate-limiting transition state for the dehydrogenation and demethylation channels. We also measured the kinetic energy release distributions (KERDs) for  $H_2$  loss from  $Ti^+(C_3H_8)$  and  $V(C_3H_8)^+$  and modeled them using statistical phase space theory.<sup>17,18</sup> This experiment probes the potential energy surface in the region of the exit channel and allows a determination of the  $Ti^+-C_3H_6$  and  $V^+-C_3H_6$  bond energies.

## Experimental Section

The metastable KERDs were measured at UCSB using a reverse geometry double focusing mass spectrometer (VG Instruments ZAB-2F)<sup>19</sup> with a home-built variable temperature EI/CI source. Metal ions were formed by electron impact (150 eV) on  $VOCl_3$  and  $TiCl_4$ . Typical source pressures were  $10^{-3}$  Torr, and source temperatures were 300 K. The nascent  $M^+-C_3H_8$  collision complexes were formed in the ion source by reaction of the bare metal ions with propane. The ion source was operated at near field free conditions to prevent kinetic excitation of the ions. The ions were accelerated to 8 kV after leaving the source and mass analyzed using a magnetic sector. Metastable ions decomposing in the second field free region between the magnetic and electric sectors were energy analyzed by scanning the electric sector. The metastable  $M^+-C_3H_8$  reactant ions contributing to the KERD are those which decompose between 5 and 15  $\mu s$  after exiting the ion source. Ions decomposing in this time window correspond to  $M^+-C_3H_8$  complexes formed from ground-state  $V^+$  and  $Ti^+$  reactant ions.<sup>20</sup> The metastable peaks were collected with a multichannel analyzer and differentiated to yield kinetic energy release distributions.<sup>21</sup> Integrated peak areas were used to obtain the product distributions. The energy resolution of the main beam was sufficient to avoid any substantive contribution to the metastable peak widths.

The ion beam results were obtained on the Utah guided ion beam apparatus, which has been described in detail previously.<sup>22</sup> A flow

tube source<sup>23</sup> is used to generate both  $Ti^+$  and  $V^+$ . Metal ions are produced by Ar ion (generated in a 1.5–3.0 keV dc discharge) sputtering of a cylindrical rod (1.25 cm in diameter and 2.5 cm in length) made of titanium or vanadium. The ions are then swept down a 1 m long flow tube by He and Ar flow gases maintained at pressures of 0.50 and 0.05 Torr, respectively. Under these conditions, the ions are calculated to undergo  $\sim 10^5$  collisions with He and  $\sim 10^4$  collisions with Ar before exiting the flow tube. Small amounts of methane were added to the flow gases to quench residual excited states. Diagnostic experiments indicate that the  $V^+$  and  $Ti^+$  beams comprise >97% ground-state ions.<sup>24</sup> The ions are focused into a magnetic sector for mass analysis, decelerated to a desired kinetic energy, and injected into an octopole ion guide. The octopole passes through a static gas cell into which the reactant gas is introduced. Pressures are maintained at a sufficiently low level (<0.1 mTorr) that multiple ion–molecule collisions are improbable. Product and unreacted metal ions are contained in the guide until they leave the gas cell. The ions are then focused into a quadrupole mass filter for product mass analysis and detected by means of a scintillation ion counter. Raw ion intensities are converted to absolute cross-sections as described previously.<sup>22</sup>

The absolute energy and the energy distribution of the reactant metal ions are measured by using the octopole as a retarding field analyzer. The full width at half-maximum of the energy distribution is generally 0.5 eV in the laboratory frame for these reactions. Uncertainties in the absolute energy scale are  $\pm 0.05$  eV lab. Translational energies in the laboratory frame of reference are related to energies in the center of mass (CM) frame by  $E_{CM} = E_{lab}m/(M + m)$ , where  $M$  and  $m$  are the masses of the incident ion and neutral reactant, respectively.

All compounds were obtained commercially and admitted to the mass spectrometer after several freeze–pump–thaw cycles to remove noncondensable gases. The deuterated hydrocarbons were obtained from Merck, Sharpe, and Dohme. The stated minimum isotopic purities were 98% for all the labeled propanes except for  $CD_3CD_2CD_3$  which was 99% pure.

## Results

Absolute cross-section measurements were obtained using a guided ion beam apparatus<sup>22</sup> for reactions of  $Ti^+$  and  $V^+$  with propane, propane-2,2-d<sub>2</sub>, propane-1,1,1,3,3,3-d<sub>6</sub>, and propane-d<sub>8</sub>. The results as a function of kinetic energy are shown in Figure 1. The total cross-sections measured at the lowest energy, 0.05 eV, are listed in Table 1 along with the reaction efficiencies ( $\sigma_{tot}/\sigma_{LGS}$ ), where  $\sigma_{LGS}$  is the Langevin–Gioumousis–Stevenson capture theory cross-section<sup>25</sup> and  $\sigma_{tot}$  the total reaction cross-section. The efficiencies are clearly low, 11–19% for  $Ti^+$  and less than 1% for  $V^+$ . For both metals,

(20) (a) Even though electronically excited-state metal ions of  $V^+$  and  $Ti^+$  will be formed by electron impact on  $VOCl_3$  and  $TiCl_4$ , only ground-state  $V^+$  and  $Ti^+$  contribute to the  $H_2$  loss KERDs from  $Ti^+(C_3H_8)$  or  $V^+(C_3H_8)$ . The cross-section data indicate ground-state  $V^+$  dehydrogenates  $C_3H_8$  exothermically. In modeling the KERD for  $H_2$  loss assuming ground-state  $V^+$  reacts with  $C_3H_8$ , we obtain a reaction exothermicity of 3 kcal/mol. Even the lowest lying excited state of  $V^+$  is 8.37 kcal/mol above ground-state  $V^+$ . Thus, this or any higher lying states of  $V^+$  cannot be contributing substantially to the  $H_2$  loss KERD observed. Similar arguments hold for  $Ti^+$  reacting with  $C_3H_8$ . Modeling the  $H_2$  loss KERD assuming ground-state  $Ti^+$  reacts with  $C_3H_8$  yields a reaction exothermicity of 7 kcal/mol. Thus, all the excited states of  $Ti^+$  above the first excited state are too high in energy to be contributing substantially to the  $H_2$  loss KERD observed. Ion chromatography has shown the first excited state of  $Ti^+$  ( $^4F$ ,  $3d^3$ ) rapidly deactivates to ground-state  $Ti^+$  even on collision with helium.<sup>20b</sup> This result is consistent with rapid deactivation of  $Ti^+(^4F, 3d^3)$  to ground-state  $Ti^+$ , in its reaction with propane, especially when competing with the tight transition state needed for product formation. (b) Kemper, P. R.; Bowers, M. T. *J. Phys. Chem.* **1991**, *95*, 5134.

(21) (a) Jarrold, M. F.; Illies, A. J.; Bowers, M. T. *Chem. Phys.* **1982**, *65*, 19. (b) Kirchner, N. J.; Bowers, M. T. *J. Phys. Chem.* **1987**, *91*, 2573.

(22) Ervin, K. M.; Armentrout, P. B. *J. Chem. Phys.* **1985**, *83*, 166.

(23) Schultz, R. H.; Armentrout, P. B. *Int. J. Mass Spectrom. Ion Processes* **1991**, *121*, 121.

(24) Sievers, M. R.; Armentrout, P. B. Manuscript in preparation.

(25) Gioumousis, G.; Stevenson, D. P. *J. Chem. Phys.* **1958**, *29*, 294.

(16) MacTaylor, R. S.; Vann, W. D.; Castleman, A. W., Jr. *J. Phys. Chem.* **1996**, *100*, 5329.

(17) (a) Pechukas, P.; Light, J. C.; Rankin, C. *J. Chem. Phys.* **1966**, *44*, 794. (b) Nikitin, E. *Theor. Exp. Chem. (Eng. Transl.)* **1965**, *1*, 285.

(18) (a) Chesnavich, W. J.; Bowers, M. T. *J. Am. Chem. Soc.* **1976**, *98*, 8301. (b) Chesnavich, W. J.; Bowers, M. T. *J. Chem. Phys.* **1978**, *68*, 901.

(c) Chesnavich, W. J.; Bowers, M. T. *Prog. React. Kinet.* **1982**, *11*, 137.

(19) Morgan, R. P.; Benyon, J. H.; Bateman, R. H.; Green, B. N. *Int. J. Mass Spectrom. Ion Phys.* **1978**, *28*, 171.

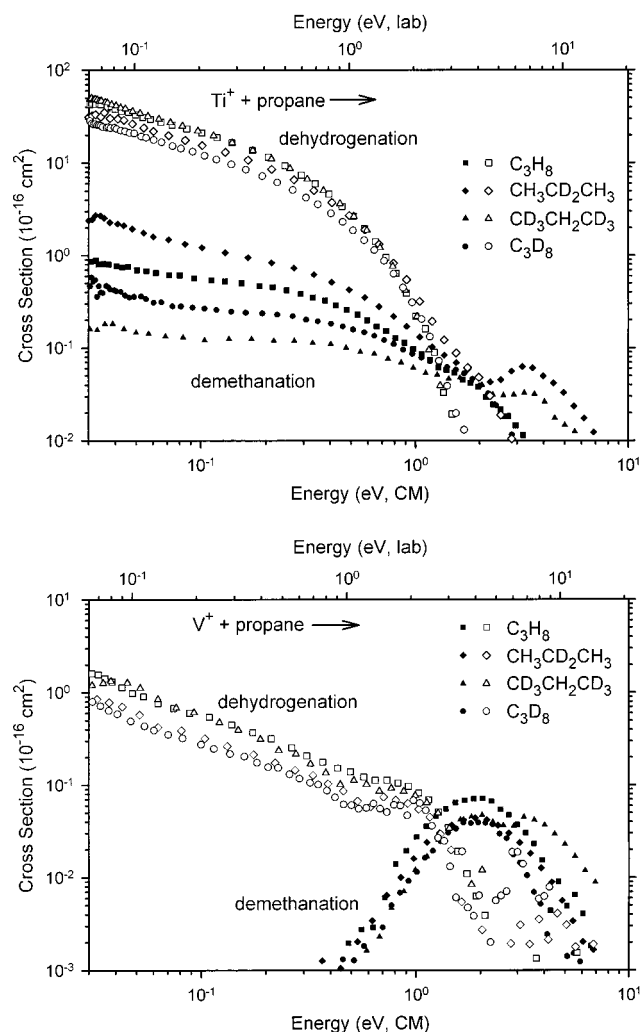


**Figure 1.** Variation of total cross-section for dehydrogenation and demethanation as a function of kinetic energy in the center-of-mass frame for the reaction of (a, top)  $\text{Ti}^+$  and (b, bottom)  $\text{V}^+$  with propane (squares), propane-2,2- $d_2$  (diamonds), propane-1,1,1,3,3,3- $d_6$  (triangles), and propane- $d_8$  (circles).

**Table 1.** Total Cross-Sections and Reaction Efficiencies for  $\text{Ti}^+$  and  $\text{V}^+$  Reacting with Isotopically Substituted Propanes under Single-Collision Conditions

| system                              | Ti                                     |                                               | V                                      |                                               |
|-------------------------------------|----------------------------------------|-----------------------------------------------|----------------------------------------|-----------------------------------------------|
|                                     | $\sigma_{\text{tot}} (\text{\AA}^2)^a$ | $(\sigma_{\text{tot}}/\sigma_{\text{LGS}})^b$ | $\sigma_{\text{tot}} (\text{\AA}^2)^a$ | $(\sigma_{\text{tot}}/\sigma_{\text{LGS}})^b$ |
| $\text{C}_3\text{H}_8$              | $33.1 \pm 3$                           | $0.18 \pm 0.02$                               | $0.98 \pm 0.2$                         | $0.005_2 \pm 0.001$                           |
| $\text{CH}_3\text{CD}_2\text{CH}_3$ | $26.6 \pm 3$                           | $0.14 \pm 0.02$                               | $0.53 \pm 0.2$                         | $0.003_8 \pm 0.001$                           |
| $\text{CD}_3\text{CH}_2\text{CD}_3$ | $36.2 \pm 3$                           | $0.19 \pm 0.02$                               | $1.25 \pm 0.2$                         | $0.006_6 \pm 0.001$                           |
| $\text{C}_3\text{D}_8$              | $21.4 \pm 3$                           | $0.11 \pm 0.02$                               | $0.49 \pm 0.2$                         | $0.003_6 \pm 0.001$                           |

<sup>a</sup> Total cross-section for methane and dihydrogen elimination measured at 0.05 eV. Propane adduct not included. <sup>b</sup> LGS is the Langevin–Gioumousis–Stevenson collision cross-section.

deuteration at the central carbon decreases the total reaction efficiencies while deuteration at the terminal carbons has little effect (possibly a slight enhancement) on the total reaction efficiencies.

Branching ratios at the lowest energy, 0.05 eV, for methane and hydrogen elimination are listed in Table 2 for various isotopomers of propane. For  $\text{Ti}^+$  reacting with  $\text{C}_3\text{H}_8$  and  $\text{C}_3\text{D}_8$ , dehydrogenation is favored over demethanation, with methane elimination accounting for only 2% of the products. Selective deuteration at the end carbons,  $\text{CD}_3\text{CH}_2\text{CD}_3$ , results in a decrease in demethanation relative to dehydrogenation. In

**Table 2.** Branching Ratios for Reactions of  $\text{Ti}^+$  and  $\text{V}^+$  with Isotopically Substituted Propanes under Single-Collision Conditions<sup>a</sup>

| $\text{M}^+$  | neutral products      | $\text{C}_3\text{H}_8$ | $\text{CH}_3\text{CD}_2\text{CH}_3$ | $\text{CD}_3\text{CH}_2\text{CD}_3$ | $\text{C}_3\text{D}_8$ |
|---------------|-----------------------|------------------------|-------------------------------------|-------------------------------------|------------------------|
| $\text{Ti}^+$ | $\text{CH}_4$         | 2                      | 5                                   |                                     |                        |
|               | $\text{CH}_3\text{D}$ |                        | 2                                   |                                     |                        |
|               | $\text{CD}_3\text{H}$ |                        |                                     |                                     | 0.2                    |
|               | $\text{CD}_4$         |                        |                                     |                                     | 0.2                    |
|               | $\text{H}_2$          | 98                     | 4                                   | 4                                   |                        |
|               | $\text{HD}$           |                        | 87                                  | 90                                  |                        |
|               | $\text{D}_2$          |                        | 2                                   | 6                                   | 98                     |
| $\text{V}^+$  | $\text{H}_2$          | 100                    | 2                                   | 2                                   |                        |
|               | $\text{HD}$           |                        | 93                                  | 91                                  |                        |
|               | $\text{D}_2$          |                        | 5                                   | 8                                   | 100                    |

<sup>a</sup> Measurements taken at 0.05 eV. Demethanation was not observed at this energy for  $\text{V}^+$ .

contrast, selective deuteration at the central carbon,  $\text{CH}_3\text{CD}_2\text{CH}_3$ , enhances demethanation. Dehydrogenation appears to favor 1,2-elimination with small but nonnegligible amounts of the other processes. For the  $\text{V}^+$ /propane system, only dehydrogenation is observed at low energies, while demethanation is observed to have an apparent threshold near 0.5 eV (Figure 1b). Deuterating the end carbons,  $\text{CD}_3\text{CH}_2\text{CD}_3$ , has no effect on the dehydrogenation cross-section relative to that observed for  $\text{V}^+$  reacting with  $\text{C}_3\text{H}_8$ . However, deuteration of the central carbon,  $\text{CH}_3\text{CD}_2\text{CH}_3$ , as well as complete deuteration,  $\text{C}_3\text{D}_8$ , reduces the dehydrogenation cross-section. Even though demethanation is not observed at low energies, an H/D isotope effect is observed for this channel. The cross-section for methane loss is highest for  $\text{C}_3\text{H}_8$  through most of the energy range examined and lower for the deuterated propanes (Figure 1b). For  $\text{C}_3\text{H}_8$  and  $\text{CH}_3\text{CD}_2\text{CH}_3$ , analysis of the demethanation thresholds yields 0 K measurements of  $0.70 \pm 0.06$  eV, whereas for  $\text{CD}_3\text{CH}_2\text{CD}_3$  and  $\text{C}_3\text{D}_8$ , they are both found to be significantly higher,  $0.82 \pm 0.06$  eV.<sup>26</sup> At the highest energies, the cross-sections for different propanes diverge strongly in several cases. These differences can be explained by alternate products having the same mass or similar mass.<sup>27</sup>

Experimental KERDs for  $\text{H}_2$  loss from  $\text{Ti}^+(\text{propane})$  and  $\text{V}^+(\text{propane})$  complexes are shown in Figure 2. The KERDs peak at low energy and fall off smoothly at higher energies, suggestive of statistical processes with no reverse activation energy in the exit channels. Statistical phase space theory is used to model the experimental KERDs for HD loss from  $\text{Ti}^+(\text{CH}_3\text{CD}_2\text{CH}_3)$  and  $\text{H}_2$  loss from  $\text{V}^+(\text{C}_3\text{H}_8)$ . (See the Appendix for details.) The resulting theoretical and experimental KERDs are compared in Figure 2. The experimental and theoretical average kinetic energy releases for HD loss from  $\text{Ti}^+(\text{CH}_3\text{CD}_2\text{CH}_3)$  are 0.067 and 0.065 eV, respectively, and for  $\text{H}_2$  loss from  $\text{V}^+(\text{C}_3\text{H}_8)$ , they are 0.049 and 0.048 eV, respectively. The theoretical KERDs shown in Figure 2 include a tight transition state along the reaction coordinate somewhere between the electrostatic well (associated with the  $\text{M}^+(\text{C}_3\text{H}_8)$  complex) and the exit channel. These fits are not sensitive to the energies of the transition states, their frequencies, or other

(26) Analysis of these thresholds is performed as detailed in many previous papers. See for example: Tjelta, B. L.; Armentrout, P. B. *J. Am. Chem. Soc.* **1996**, *118*, 9652. Haynes, C. L.; Fisher, E. R.; Armentrout, P. B. *J. Phys. Chem.* **1996**, *100*, 18300.

(27) In the demethanation channels for both metals, the high-energy features in the  $\text{M}^+(\text{C}_2\text{H}_2\text{D}_2)$  products observed for the  $\text{C}_3\text{H}_2\text{D}_6$  system are attributable to a  $\text{M}^+(\text{C}_2\text{D}_3)$  product having the same mass. In the  $\text{Ti}^+ + \text{C}_3\text{H}_6\text{D}_2$  system, the high-energy feature in the  $\text{M}^+(\text{C}_2\text{H}_2\text{D}_2)$  product is probably  $\text{Ti}^+(\text{C}_2\text{HD}_2)$  and that for  $\text{Ti}^+(\text{C}_3\text{H}_5\text{D})$  is probably  $\text{Ti}^+(\text{C}_3\text{H}_2\text{D}_2)$ , one mass unit lower. Data acquired for this latter system were taken at somewhat lower mass resolution than those for the other systems.

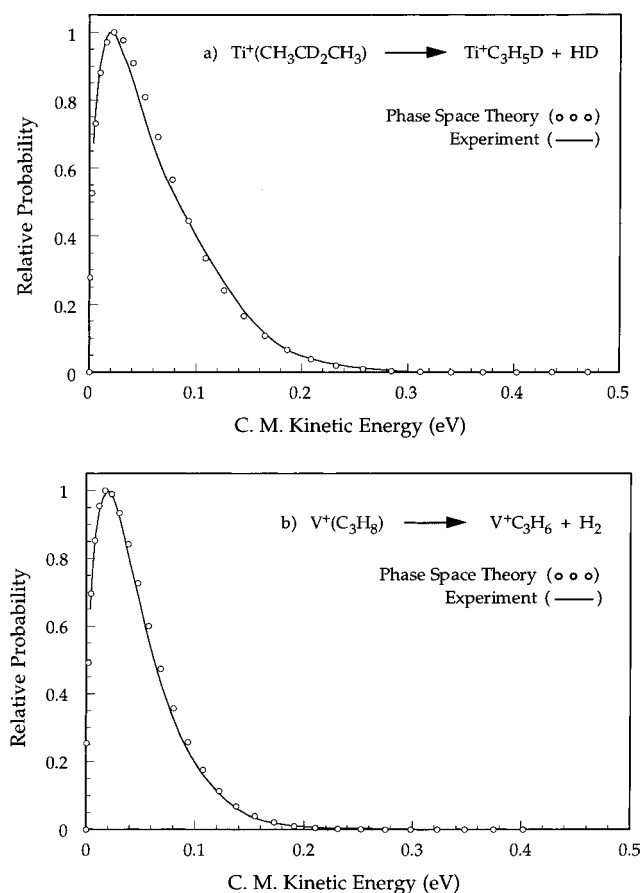
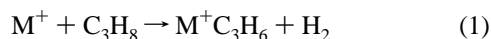


**Figure 2.** Kinetic energy release distribution for metastable loss of  $H_2$  from nascent (a, top)  $Ti^+(C_3H_8)$  and (b, bottom)  $V^+(C_3H_8)$  collision complexes. The solid line labeled "experiment" results from analysis of the laboratory peak shape using standard techniques.<sup>21</sup> The circles are the results of statistical phase space calculations as described in the text.

parameters in the calculations. In fact, the average kinetic energy release calculated is identical to that calculated without the tight transition state. However, if the tight transition state is not included in the model, slight changes in the shape of the distribution are observed. Specifically, the model distributions peak at slightly higher energies and fall off more quickly as energy increases. Previous studies<sup>4</sup> have shown that including a tight transition state in the model induces a significant angular momentum restriction (reducing the average kinetic energy released) for methane elimination from  $M^+$ (propane) complexes when  $M = Fe, Co,$  and  $Ni$ .<sup>4,5</sup> However, inclusion of the barrier does not significantly restrict the angular momentum for  $H_2$  loss from the  $M^+(C_3H_8)$  complex because this process is already restricted to low angular momenta, due to the low mass and polarizability of  $H_2$ . Hence, only minor changes in the KERD are observed by inclusion of the barrier. In the present study, we were unable to measure the KERD for methane loss from  $Ti^+(C_3H_8)$  due to the low efficiency for this reaction.

In the calculation of the model KERDs, the only parameter allowed to freely vary was  $\Delta_{rxn}H_0^\circ$  of reaction 1. The optimal



enthalpies of reaction, which yield the fits shown in Figure 2, are  $-7 \pm 3$  and  $-3 \pm 2$  kcal/mol for  $M = Ti$  and  $V$ , respectively. As all species in reaction 1 have known heats of formation except  $M^+ - C_3H_6$ , the optimum values found allow

us to determine  $D_0^\circ(Ti^+ - C_3H_6) = 34.5 \pm 3$  kcal/mol and  $D_0^\circ(V^+ - C_3H_6) = 30.7 \pm 2$  kcal/mol.

## Discussion

**A. Energetics of the Dehydrogenation and Demethanation Reactions.** The  $Ti^+ - C_3H_6$  and  $V^+ - C_3H_6$  bond energies (at 0 K) of  $34.5 \pm 3$  and  $30.7 \pm 2$  kcal/mol, respectively, obtained by modeling the experimental KERDs with statistical phase space theory can be compared with recent experimentally determined  $M^+ - C_2H_4$  bond energies of  $34.8 \pm 2.5$  and  $29.7 \pm 1.8$  kcal/mol, respectively.<sup>28,29</sup> The latter are expected to be slightly lower because the polarizability of  $C_2H_4$  is smaller than that of  $C_3H_6$ . Theoretical studies<sup>30</sup> yield metal ion-ethene bond energies ( $D_e$  values) of 24.2 and 25.2 kcal/mol for  $Ti^+(C_2H_4)$  and  $V^+(C_2H_4)$ , respectively. The authors note that these values are expected to be too low and suggest corrections of 7–9 kcal/mol for the covalently bound  $Ti^+(C_2H_4)$  and 3–5 kcal/mol for the electrostatically bound  $V^+(C_2H_4)$ . This gives final theoretical values at 0 K of  $31 \pm 1$  and  $28 \pm 1$  kcal/mol, respectively, in reasonable agreement with experiment.

The metal ion-propene bond energies measured here indicate that the  $H_2$  elimination reactions from propane are only modestly exothermic at 0 K:  $7 \pm 3$  kcal/mol for  $Ti^+ + C_3H_8$  and  $3 \pm 2$  kcal/mol for  $V^+ + C_3H_8$ .<sup>31</sup> Methane elimination is considerably more exothermic on the basis of the metal ion-ethene bond energies measured in CID studies:  $16 \pm 3$  kcal/mol for  $Ti^+ + C_3H_8$  and  $11 \pm 2$  kcal/mol for  $V^+ + C_3H_8$ .<sup>28</sup>

**B. Reaction Cross-Sections for  $Ti^+$  and  $V^+$  Reacting with Propane.** As discussed in the previous section, dehydrogenation and demethanation of propane by  $Ti^+$  are exothermic processes. The shapes of the energy dependent cross-sections for both product channels (Figure 1a) indicate that no barriers along the reaction coordinate exceed the asymptotic energy of the reactants. Despite this, the reactions are clearly inefficient. For  $Ti^+ + C_3H_8$ , the absolute cross-section for  $H_2$  loss at 0.05 eV corresponds to a rate constant of  $2.1 \pm 0.4 \times 10^{-10}$  cm<sup>3</sup>/s. This value is lower than the dehydrogenation rate constants of  $6.4 \pm 2 \times 10^{-10}$  and  $6.2 \pm 1.9 \times 10^{-10}$  cm<sup>3</sup>/s obtained under high-pressure multicollision conditions by Tonkyn et al.<sup>12</sup> and MacTaylor et al.,<sup>16</sup> respectively. The reaction efficiency under single collision conditions at 0.05 eV (reported here) is 17% for  $H_2$  loss and less than 1% for  $CH_4$  loss. Thus, 82% of the collision complexes formed go back to reactants. In the high pressure of the flow tube, only 63% of the collision complexes return to reactants.<sup>12</sup> Thus, it appears that some of the transiently formed  $(Ti^+C_3H_8)^*$  complexes collide with He before dissociating back to reactants or going on to products. These collisions can stabilize these complexes, eliminating the back-reaction but allowing some of them to react to form products. The observation that a higher rate of adduct formation was

(28) Sievers, M. R.; Jarvis, L. M.; Armentrout, P. B. *J. Am. Chem. Soc.*, submitted for publication.

(29) Armentrout, P. B.; Kickel, B. L. In *Organometallic Ion Chemistry*; Freiser, B. S., Ed.; Kluwer Academic Publishers: The Netherlands, 1996; p 1.

(30) (a) Sodupe, M.; Bauschlicher, C. W.; Langhoff, S. R.; Partridge, H. *J. Phys. Chem.* **1992**, *96*, 2118. (b) Sodupe, M.; Bauschlicher, C. W. *J. Phys. Chem.* **1991**, *95*, 8645. (c) Bauschlicher, C. W. In *Organometallic Ion Chemistry*; Freiser, B. S., Ed.; Kluwer Academic Publishers: Dordrecht, The Netherlands, 1996.

(31) Literature thermochemistry for stable hydrocarbons is taken from the following: (a) Pedley, J. B.; Naylor, R. D.; Kirby, S. P. *Thermochemical Data of Organic Compounds*, 2nd ed.; Chapman and Hall: New York, 1986. Correction to 0 K values is achieved using information in the following: Chase, M. W., Jr.; Davies, C. A.; Downey, J. R., Jr.; Frurip, D. J.; McDonald, R. A.; Syverud, A. N. *J. Phys. Chem. Ref. Data* **1985**, *14* (No. 1). (b) Lias, S. G.; Bartmess, J. E.; Liebman, J. F.; Holmes, J. L.; Levin, R. D.; Mallard, W. G. *J. Phys. Chem. Ref. Data* **1988**, *17*, Suppl. 1.

observed at 0.75 Torr ( $1.2 \pm 0.4 \times 10^{-10}$  cm<sup>3</sup>/s)<sup>12</sup> than at 0.2–0.6 Torr ( $0.5 \pm 0.2 \times 10^{-10}$  cm<sup>3</sup>/s)<sup>16</sup> is consistent with this hypothesis. Note also that the initial energy distribution for the reactants under the high-pressure conditions of the flow tube (a Boltzmann distribution at 300 K) differs somewhat from that of the ion beam work at 0.05 eV. This could also affect the relative efficiencies observed for the forward reaction.

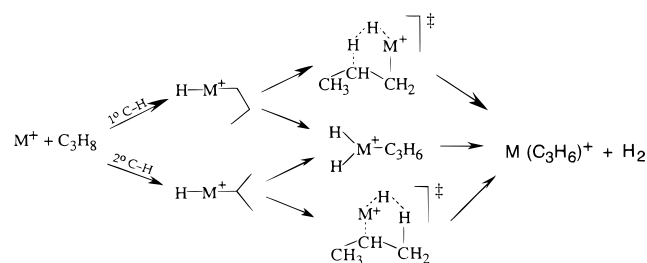
For V<sup>+</sup> reacting with propane, dehydrogenation and demethanation channels are both exothermic but slightly less so than for Ti<sup>+</sup>. Again no sign of a barrier exceeding the reaction threshold energy is found in the cross-section data for dehydrogenation. However, as shown in Figure 1b, the threshold observed in the cross-section for methane elimination (the more exothermic reaction) indicates a barrier of about 0.7 eV above the energy of the reactants. Even though exothermic and barrierless, the absolute cross-section for H<sub>2</sub> loss at 0.05 eV corresponds to a rate constant of only  $1.0 \pm 0.2 \times 10^{-11}$  cm<sup>3</sup>/s. In the high-pressure, flow tube environment, Tonkyn et al. measure a dehydrogenation rate constant of  $2.8 \times 10^{-11}$  cm<sup>3</sup>/s, again somewhat larger than the value determined in this study. In the vanadium system, adduct formation in the high-pressure flow tube is even more efficient than in the Ti<sup>+</sup> system, occurring at a rate of  $4.4 \pm 1.3 \times 10^{-10}$  cm<sup>3</sup>/s. Under single-collision conditions, 99.5% of the collision complexes return to reactants, while at 0.75 Torr of He, only 76% do.

The observations of inefficient reactions without energetic restrictions point to a potential energy surface in which there is a rate-limiting transition state along the reaction coordinate. The closer in energy this transition state is to the asymptotic energy of the reactants, the less efficient the reaction should be. Alternatively, when the reactants do not conserve spin with the intermediates or products, the efficiency of reaction could be limited by the coupling between surfaces of different spin multiplicity. Finally, a combination of these effects could be occurring either independently or in a situation where surface coupling is efficient but the required surface crossing energy is high enough that it corresponds to the rate-limiting point along the potential energy surface. These options will be discussed below.

**C. Reaction Efficiencies for Ti<sup>+</sup> and V<sup>+</sup> Reacting with Labeled Propanes.** The cross-sections for dehydrogenation of CH<sub>3</sub>CD<sub>2</sub>CH<sub>3</sub> and C<sub>3</sub>D<sub>8</sub> by both Ti<sup>+</sup> and V<sup>+</sup> are substantially less than that for C<sub>3</sub>H<sub>8</sub>. In contrast, the cross-section for dehydrogenation of CD<sub>3</sub>CH<sub>2</sub>CD<sub>3</sub> is essentially equivalent to that for C<sub>3</sub>H<sub>8</sub> in both systems. The selective deuteration results indicate that breaking a secondary C–H bond is a primary contributor to the dehydrogenation transition state in both metal systems.

Likewise, the demethanation channel is strongly affected by deuteration. In the titanium system, the cross-section for demethanation from CD<sub>3</sub>CH<sub>2</sub>CD<sub>3</sub> is reduced by a factor of about 5 relative to that from C<sub>3</sub>H<sub>8</sub>. Deuteration at the central carbon enhances methane elimination by a factor of about 2–3 relative to that from C<sub>3</sub>H<sub>8</sub>. In the vanadium system, the magnitudes of the cross-sections for methane loss are more similar but do exhibit different thresholds. Here, the thresholds measured for methane loss from C<sub>3</sub>H<sub>8</sub> and CH<sub>3</sub>CD<sub>2</sub>CH<sub>3</sub> are lower than those for CD<sub>3</sub>CH<sub>2</sub>CD<sub>3</sub> and C<sub>3</sub>D<sub>8</sub> by  $0.12 \pm 0.08$  eV. These observations point to activation of a terminal C–H(D) bond as being involved in the rate-limiting step for demethanation. The observation of a threshold for demethanation in the reaction of ground-state V<sup>+</sup> + C<sub>3</sub>H<sub>8</sub> (Figure 1b) is consistent with the results of Sanders et al.<sup>8</sup> They observed that the <sup>5</sup>D, 3d<sup>4</sup> ground state and the <sup>5</sup>F, 3d<sup>3</sup>4s first excited state of V<sup>+</sup> (~0.34 eV above the

Scheme 1



ground state) do not react with C<sub>3</sub>H<sub>8</sub> to eliminate methane at thermal energy. The presence of a significant barrier is also consistent with the inefficient reaction observed by Sanders et al.<sup>8</sup> for the <sup>3</sup>F, 3d<sup>3</sup>4s state of V<sup>+</sup> with C<sub>3</sub>H<sub>8</sub>. This state lies 1.1 eV above ground-state V<sup>+</sup> and conserves spin to activate propane, as discussed further below.

**D. 1,2-Hydrogen Elimination. The Rate-Limiting Transition State.** The observation of a single-component, statistical KERD for H<sub>2</sub> loss from Ti<sup>+</sup>(C<sub>3</sub>H<sub>8</sub>) and V<sup>+</sup>(C<sub>3</sub>H<sub>8</sub>) is consistent with a single dissociation process occurring for both metals and indicates that there is no reverse activation energy barrier present in either exit channel. Further, the fact that the cross-sections (Figure 1) smoothly and monotonically decrease with energy indicates that no other significant channels arise over the energy range sampled (0–5 eV CM). These results indicate H<sub>2</sub> loss comes dominantly from a (C<sub>3</sub>H<sub>6</sub>)M<sup>+</sup>(H<sub>2</sub>) complex (in which the H<sub>2</sub> is electrostatically bound) as the last significant feature along the reaction coordinate.

There are two primary mechanisms for dehydrogenation that have evolved in previous work and are shown in Scheme 1. Both mechanisms involve initial primary or initial secondary C–H bond activation to form hydridopropylmetal cation intermediates. In the classic “stepwise” mechanism, this oxidative addition step is followed by β-H migration to the metal to form a dihydride propene metal ion complex which can reductively eliminate H<sub>2</sub>. More recently, theoretical studies<sup>15,32</sup> have indicated that the dihydride–propene intermediate may not exist for late first-row transition metals and suggest that elimination occurs through a multicenter transition state (MCTS), bypassing the dihydride intermediate.

Evidence for a mechanism like Scheme 1 was presented in previous studies of Fe<sup>+</sup>, Co<sup>+</sup>, and Ni<sup>+</sup> reacting with propane.<sup>4,5</sup> A bimodal KERD for H<sub>2</sub> loss and an H/D isotope effect on the two components of the bimodal KERD in these systems indicated two distinct dissociation processes: one a statistical process and one a higher energy direct process. The statistical process was assumed to result from a dihydride intermediate leading to a (C<sub>3</sub>H<sub>6</sub>)M<sup>+</sup>(H<sub>2</sub>) complex which then dissociated. The high-energy process was assumed to result from H<sub>2</sub> elimination via a MCTS leading directly to products.

Although recent calculations bring the stability of the dihydride intermediate into question for the late metals,<sup>15,32</sup> this pathway may be energetically accessible for early metals and will be considered in this work. One simple way of understanding why the dihydride propene intermediate is unstable for late transition metal ions is to recognize that the metal–hydrogen bonds in the (H)M<sup>+</sup>(H) species utilize 4s–3d hybrids. For late metals (Mn–Cu), the four remaining 3d orbitals are occupied with one or two electrons such that there are no empty orbitals to accept electron density from the propene ligand. For early metals, the 4s–3d hybridization is more efficient, such that the

(32) Holthausen, M. C.; Fiedler, A.; Schwarz, H.; Koch, W. *Angew. Chem., Int. Ed. Engl.* **1995**, *34*, 2282.

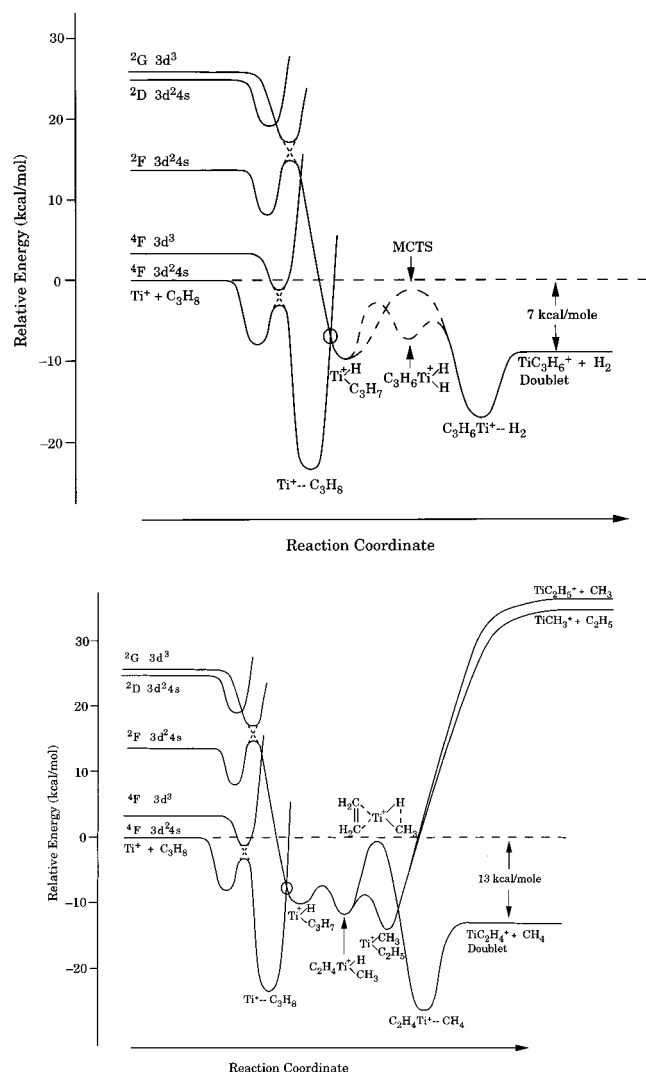


**Figure 3.** Schematic reaction coordinate diagrams for the reaction of  $\text{Ti}^+$  with propane to eliminate (a, top)  $\text{H}_2$  and (b, bottom)  $\text{CH}_4$ . The overall reaction exothermicity for  $\text{H}_2$  loss was determined in this study by modeling the experimental  $\text{H}_2$  loss KERD using statistical phase space theory. The exothermicity for  $\text{CH}_4$  loss is based on the metal ion–ethene bond energy measured in CID studies.<sup>28</sup> Energies of intermediates were estimated. For example, the  $\text{Ti}^+(\text{C}_3\text{H}_8)$  bond energy estimate is based on the measured  $\text{Ti}^+(\text{CH}_4)$  bond energy,<sup>5a</sup> and the  $(\text{H})\text{Ti}^+(\text{C}_3\text{H}_7)$  inserted intermediate bond energy was estimated from  $\text{Ti}^+-\text{H}$ ,  $\text{Ti}-\text{CH}_3$ , and  $\text{CH}_3\text{Ti}^+-\text{CH}_3$  bond energies (see the text).<sup>29,36</sup> The structures for the multicenter transition state (MCTS) are shown in Scheme 1.

$(\text{H})\text{M}^+(\text{H})$  species is more stable, and not all of the remaining 3d orbitals are occupied, such that a strong dative bond between the metal ion and propene can be formed. Thus, explicit consideration of both the stepwise and multicenter mechanisms is needed for the early-transition-metal systems.

In the present study, neither the cross-sections nor KERDs provide any indications of multiple routes for dehydrogenation. Both primary and secondary C–H bond activation can occur.<sup>10,12,28,33</sup> If initial primary C–H bond activation is the dominant contributor to the dehydrogenation reactions for  $\text{Ti}^+$  and  $\text{V}^+$  reacting with propane, the observed H/D isotope effect in the cross-section data indicates that the rate-limiting transition state is associated with the  $\beta$ -H(D) transfer step or multicenter elimination step of Scheme 1. In the stepwise mechanism, the

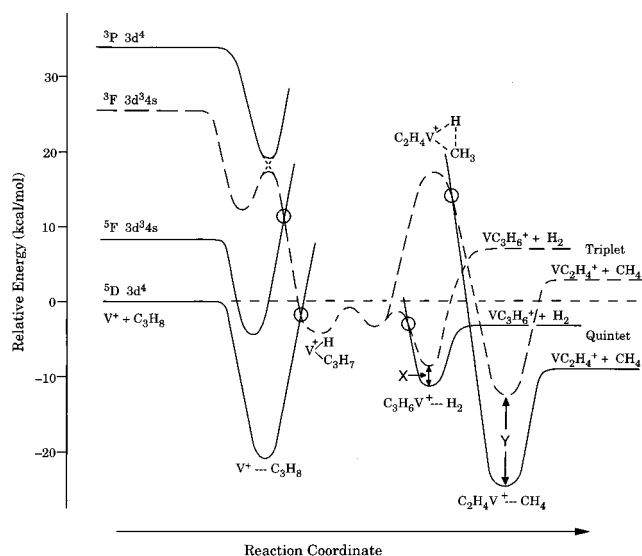


**Figure 4.** Schematic reaction coordinate diagram for the reaction of  $\text{V}^+$  ( $^3\text{D}$ ,  $3\text{d}^4$ ) and  $\text{V}^+$  ( $^3\text{F}$ ,  $3\text{d}^34\text{s}$ ) with propane to eliminate  $\text{H}_2$  and  $\text{CH}_4$ . The triplet surface is dashed, and the quintet surface is solid. X and Y correspond to the energies of the triplet–quintet splitting for  $(\text{C}_3\text{H}_6)\text{V}^+-\text{H}_2$  and  $(\text{C}_2\text{H}_4)\text{V}^+-\text{CH}_4$ , respectively. The overall reaction exothermicity for  $\text{H}_2$  loss was determined in this study by modeling the experimental  $\text{H}_2$  loss KERD using statistical phase space theory. The exothermicity for  $\text{CH}_4$  loss is based on the metal ion–ethene bond energy measured in CID studies.<sup>28</sup> Energies of intermediates were estimated. For example, the  $(\text{H})\text{V}^+(\text{C}_3\text{H}_7)$  inserted intermediate was estimated from  $\text{V}^+-\text{H}$ ,  $\text{V}^+-\text{CH}_3$ , and  $\text{CH}_3\text{V}^+-\text{CH}_3$  bond energies (see the text).<sup>29,36</sup>

$\text{H}_2$  elimination step associated with an H–H(D) coupling transition state is probably not rate-limiting; otherwise we would expect to observe more extensive H/D scrambling (Table 2). On the other hand, if initial secondary C–H bond activation is occurring, then the rate-determining step must be the initial insertion in order to explain the observed isotope effects. It is likely both primary and secondary C–H bond activation are occurring, but both statistical factors (six primary C–H bonds versus two secondary) and the data for methane loss (see below) indicate primary C–H bond insertion dominates the observed reactivity.

The question of how spin might affect the reaction is addressed as follows. Both metal ions have high-spin ground states:  $^4\text{F}$ ,  $4\text{s}3\text{d}^2$  for  $\text{Ti}^+$  and  $^5\text{D}$ ,  $3\text{d}^4$  for  $\text{V}^+$ . The initial step in all mechanisms involves formation of a  $\text{H}-\text{M}^+-\text{C}_3\text{H}_7$  intermediate. Both the  $\text{M}^+-\text{H}$  and  $\text{M}^+-\text{C}_3\text{H}_7$  bonds are covalent and presumed to be formed with  $4\text{s}-3\text{d}$  hybrid orbitals on the metal ion. The remaining unpaired electron(s) on the metal occupy the remaining four 3d orbitals such that, for  $\text{Ti}^+$  and  $\text{V}^+$ , the spins of the  $\text{H}-\text{M}^+-\text{C}_3\text{H}_7$  ground-state intermediates are doublet and triplet, respectively. Thus, formation of the initial  $\text{H}-\text{M}^+-\text{C}_3\text{H}_7$  intermediate for both  $\text{Ti}^+$  and  $\text{V}^+$  requires a spin–orbit-coupled crossing from the surface of the separated ground-state  $\text{M}^+ + \text{C}_3\text{H}_8$  reactants. Because both systems eliminate  $\text{H}_2$  at thermal energies and there is no evidence for a barrier in the cross-section data, these crossings must occur below the reactant asymptotic energies as shown in Figures 3 and 4.

In the case of  $\text{Ti}^+$ , the most stable products are doublets,<sup>30</sup> so no further spin changes are implied during the  $\text{H}_2$  (and  $\text{CH}_4$ ) elimination steps. Significant isotope effects are observed in the  $\text{Ti}^+$  cross-section at low energies, while spin–orbit crossings are expected to have little or no isotopic dependence. This indicates that the energy of the transition state plays an important

(33) Tolbert, M. A.; Beauchamp, J. L. *J. Am. Chem. Soc.* **1986**, *108*, 7509.

role in determining the overall reaction efficiency. At present the role of spin-orbit coupling in determining reaction efficiency cannot be assessed.

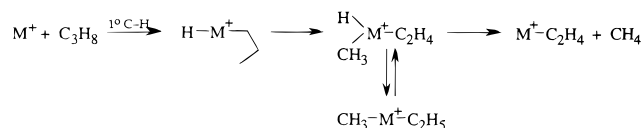
Similar arguments apply to H<sub>2</sub> loss in the V<sup>+</sup>/C<sub>3</sub>H<sub>8</sub> reaction. In this instance, there are two surface crossings required because the reaction starts on the quintet surface, crosses to the triplet surface on initial C-H insertion, and then returns to the quintet surface because only the quintet products yield an overall exoergic reaction. Here too, the isotope effects clearly indicate that the energy of the transition state plays a critical role in the observed reaction efficiency. Even though there is no direct evidence regarding the role of the two spin-orbit crossings in determining the reaction efficiency, it is plausible that these are in part responsible for the lower reaction efficiency of V<sup>+</sup> relative to that of Ti<sup>+</sup>.

The effect of spin on reaction rates has been observed.<sup>8</sup> If the system is initiated on excited-state surfaces with the same spin as the products, then rates can be enhanced. For example, electronically excited low-spin Ti<sup>+</sup> and V<sup>+</sup> are 10–100 times more reactive with propane than their high-spin ground states,<sup>8</sup> but in this instance it is not clear whether favorable spin or the substantial increase in energy or both are responsible for the increased reaction efficiency. However, the fact that the <sup>5</sup>F state of V<sup>+</sup> does not show enhanced reactivity relative to the <sup>5</sup>D state of V<sup>+</sup> reacting with propane<sup>8</sup> despite its 0.34 eV greater energy<sup>34</sup> suggests some factor other than energy must be involved in the rate determination. Conservation of spin is a likely candidate.

**E. Methane Elimination. The Rate-Limiting Transition State.** We consider several possible mechanisms for the reactions of Ti<sup>+</sup> and V<sup>+</sup> with propane to eliminate methane. The initial steps can involve either primary C-H(D) or C-C bond activation. If the first step in this reaction is initial primary C-H(D) bond activation, then the rate-limiting step for demethanation of propane by M<sup>+</sup> could be associated with the methyl transfer step, the subsequent methane elimination step involving C-H(D) coupling, or a MCTS that would involve coupling the methyl group with the primary H(D) atom on the metal ion. We dismiss the methyl transfer step as rate limiting because it involves only C-C bond cleavage and M-C bond formation such that no strong deuterium isotope effects are expected. Isotope effects are expected for either initial primary C-H(D) activation followed by C-H(D) coupling in the methane elimination step from a (C<sub>2</sub>H<sub>4</sub>)M<sup>+</sup>(H)(CH<sub>3</sub>) intermediate or through a MCTS from a (H)M<sup>+</sup>(1-C<sub>3</sub>H<sub>7</sub>) intermediate. If demethanation starts with initial C-C bond activation, strong deuterium isotope effects are not expected if this insertion step is rate limiting. However, if the subsequent β-H(D) transfer step to form (C<sub>2</sub>H<sub>4</sub>)M<sup>+</sup>(H)(CH<sub>3</sub>) or a multicenter elimination of methane from (CH<sub>3</sub>)M<sup>+</sup>(C<sub>2</sub>H<sub>5</sub>) is rate limiting, then isotope effects are expected.

In the case of Ti<sup>+</sup> reacting with propane, we observe a 5-fold depression of the demethanation process for CD<sub>3</sub>CH<sub>2</sub>CD<sub>3</sub> relative to C<sub>3</sub>H<sub>8</sub>. This points to the involvement of a primary hydrogen in the rate-limiting step, which is consistent with any of the pathways mentioned above. However, the mechanism must also indicate why deuteration at the central carbon enhances demethanation by a factor of 2–3. None of the mechanisms for demethanation involve the secondary hydrogens directly, such that competition with dehydrogenation must be responsible. This H/D isotope effect is most easily explained if the dehydrogenation and demethanation channels go through

## Scheme 2



a common intermediate followed by transition states where the branching ratios are determined. The only common intermediate among the various possible pathways considered for dehydrogenation and demethanation is the H-M<sup>+</sup>-1-C<sub>3</sub>H<sub>7</sub> species formed by initial primary C-H(D) bond activation. We have already concluded the H<sub>2</sub> loss rate-limiting transition state is β-H(D) transfer or a MCTS; hence, deuteration of the secondary hydrogens increases the barrier for either of these processes and could lead to increased methane loss.

In the case of V<sup>+</sup> reacting with propane, the 0.82 ± 0.06 eV threshold observed for demethanation of CD<sub>3</sub>CH<sub>2</sub>CD<sub>3</sub> and C<sub>3</sub>D<sub>8</sub> is significantly higher than the 0.70 ± 0.06 eV threshold observed for demethanation of C<sub>3</sub>H<sub>8</sub> and CH<sub>3</sub>CD<sub>2</sub>CH<sub>3</sub>. The 0.12 ± 0.08 eV difference in thresholds is reasonably consistent with the maximum difference of 0.05 eV in the transition-state energies (due to zero-point energy differences) expected for primary C-H versus C-D bond cleavage. This implies that the rate-limiting transition state must involve breaking or forming a C-H(D) bond. Because H<sub>2</sub> loss is observed at thermal energies and involves initial C-H(D) bond activation, the 0.70 eV threshold observed for demethanation cannot be associated with this transition state. Considering that demethanation of CD<sub>3</sub>CH<sub>2</sub>CD<sub>3</sub> and C<sub>3</sub>D<sub>8</sub> involves C-D coupling and that of C<sub>3</sub>H<sub>8</sub> and CH<sub>3</sub>CD<sub>2</sub>CH<sub>3</sub> involves C-H coupling, a rate-limiting C-H(D) coupling transition state from a (C<sub>2</sub>H<sub>4</sub>)M<sup>+</sup>(H)(CH<sub>3</sub>) intermediate or a MCTS from H-M<sup>+</sup>-1-C<sub>3</sub>H<sub>7</sub> near the exit channel can explain the observed H/D isotope effect.

The final observation that can help elucidate the mechanism for methane elimination is the observation of H/D scrambling for demethanation of both CD<sub>3</sub>CH<sub>2</sub>CD<sub>3</sub> and CH<sub>3</sub>CD<sub>2</sub>CH<sub>3</sub> by Ti<sup>+</sup>. Neither mechanism (stepwise or MCTS) can explain scrambling without invoking some additional species.<sup>35</sup> If it is presumed that the mechanism is stepwise, then H/D scrambling can be explained by reversible hydrogen transfers between (C<sub>2</sub>H<sub>4</sub>)M<sup>+</sup>(H)(CH<sub>3</sub>) and (CH<sub>3</sub>)M<sup>+</sup>(C<sub>2</sub>H<sub>5</sub>) intermediates (Figure 3b, Scheme 2). Complete scrambling in the ethyl group predicts CH<sub>4</sub>/CH<sub>3</sub>D and CD<sub>4</sub>/CHD<sub>3</sub> product ratios of 3/2 if movements of H and D are energetically equivalent. Because breaking a C-D bond is energetically more difficult than breaking a C-H bond, these ratios shift in favor of the less deuterated products, in line with the experimentally observed values of 5/2 for C<sub>3</sub>H<sub>6</sub>D<sub>2</sub> and 1/1 for C<sub>3</sub>H<sub>2</sub>D<sub>6</sub>.

Overall, the mechanism for demethanation most consistent with all observations is initial primary C-H bond activation, followed by methyl transfer and a rate-limiting transition state associated with reductive elimination of methane (Scheme 2). The final step in Scheme 2 is rate limiting. It seems likely that a similar mechanism is followed for both Ti<sup>+</sup> and V<sup>+</sup>.

(35) A MCTS mechanism cannot be completely ruled out. The 2% CH<sub>3</sub>D product (Table 2) could arise from initial formation of D-Ti<sup>+</sup>-2-C<sub>3</sub>H<sub>6</sub>D from CH<sub>3</sub>CD<sub>2</sub>CH<sub>3</sub> followed by CH<sub>3</sub>D loss via an MCTS to form Ti<sup>+</sup>=CDCH<sub>3</sub>. While the overall energetics of this process are not well characterized, it is possible that the ethylidene product can be formed exothermically from Ti<sup>+</sup> and propane.<sup>29,36</sup> If this process were occurring, however, one would expect a significant loss of CD<sub>3</sub>H from CD<sub>3</sub>CH<sub>2</sub>CD<sub>3</sub> which is not observed (Table 2). In fact the very favored overall loss of methane from CH<sub>3</sub>CD<sub>2</sub>CH<sub>3</sub> relative to C<sub>3</sub>H<sub>8</sub>, C<sub>3</sub>D<sub>8</sub>, and CD<sub>3</sub>CH<sub>2</sub>CD<sub>3</sub> points to initial primary C-H insertion as the dominant process for methane loss (Table 2), as previously discussed in the text. No isotope effect is expected from initial primary insertion if a MCTS is involved.

(34) (a) Moore, C. E. *Atomic Energy Levels*; Circ. 467; U.S. National Bureau of Standards: Washington, DC, 1952. (b) Sugar, J.; Corliss, C. J. *Phys. Chem. Ref. Data* **1981**, 10, 197, 1097. (c) *Ibid.* **1982**, 11, 135.

The question remains as to why elimination of methane exhibits a barrier for  $V^+$  and not for  $Ti^+$ . The answer requires that we consider the electronic states of the products. Theoretical studies of the bonding of first-row transition-metal ions to ethene<sup>30</sup> show that  $Ti^+C_2H_4$  has a  $^2A_1$  ground state in which  $Ti^+$  inserts into the  $\pi$ -bond of the ethene. There is a high-spin, electrostatically bound  $^4B_2$  excited state lying 5.2 kcal/mol higher in energy. For vanadium, the high-spin, electrostatically bound  $^5A_1$  state is the ground state of  $V^+C_2H_4$ , and the low-spin,  $^3A_2$  state lies 14.8 kcal/mol higher in energy, as shown in Figure 4. Thus, for ground-state  $Ti^+$  ( $^4F$ ,  $4s3d^2$ ) reacting with propane, a spin-orbit-coupled crossing to the doublet surface occurs to insert into the C-H bond, and subsequently the reaction remains on the doublet surface. For the reaction of ground-state  $V^+$  ( $^5D$ ,  $3d^4$ ) with propane, an analogous spin-orbit-coupled crossing to the triplet surface occurs to insert into the C-H bond, but a subsequent crossing to the quintet surface must occur to access the low-energy  $V^+C_2H_4/CH_4$  products, although formation of triplet  $V^+C_2H_4$  can occur with an estimated threshold of 3.5 kcal/mol (0.15 eV), well below the 0.7 eV barrier observed for methane elimination. Hence, the barrier observed for demethanation of propane by  $V^+$  can be attributed to either the transition state for methane elimination on the low-spin triplet surface or the energy where the quintet and triplet surfaces cross in the exit channel. Because  $H_2$  elimination does not show a barrier and it must form quintet products to be exoergic, it is likely the observed barrier associated with  $CH_4$  elimination is due to the C-H(D) coupling transition state on the triplet surface and not to a triplet/quintet surface crossing, although participation of a MCTS cannot be ruled out.

**F. Relative Reactivities of  $Ti^+$  and  $V^+$  with Propane.** The greater reactivity of  $Ti^+$  relative to  $V^+$  with propane is partially due to greater stability of intermediates and products for the titanium system. The energies of the inserted  $H-M^+-C_3H_7$  intermediates are determined by several factors: the 3d to 4s promotion energy (including the energies of the excited states, the energy of the  $Ti^+$  ( $^4F$ ,  $3d^3$ ) and  $V^+$  ( $^5F$ ,  $4s3d^3$ ) states, and the loss in d-d and s-d exchange energies) and the energies of the bonds being formed. For  $V^+$ , sd hybridization is energetically less favorable than for  $Ti^+$ , partly due to the fact that the s and d orbitals are closer in energy for titanium than for vanadium, as shown by the lower lying electronic excited states of titanium relative to vanadium (see Figures 3 and 4). From experimental bond dissociation energies<sup>29,36</sup> of  $M^+-H$ ,  $M^+-CH_3$ , and  $MCH_3^+-CH_3$ ,  $D_0(H-M^+-CH_3)$  was estimated to be  $115 \pm 6$  kcal/mol for  $M = Ti$  and  $95 \pm 4$  kcal/mol for  $M = V$ . These results are in line with those of a recent theoretical study of the stability of  $H-M^+-CH_3$  complexes of first-row transition metals where  $H-Ti^+-CH_3$  was found to be 17 kcal/mol more stable than  $H-V^+-CH_3$  relative to their respective  $M^+ + CH_4$  asymptotes.<sup>37</sup> Thus,  $H-Ti^+-C_3H_7$  is more stable than  $H-V^+-C_3H_7$ , and the formation of  $Ti^+C_2H_4 + CH_4$  and  $Ti^+C_3H_6 + H_2$  products is more exothermic than formation of  $V^+C_2H_4 + CH_4$  and  $V^+C_3H_6 + H_2$  products. Both of these factors should increase the efficiency of reaction of  $Ti^+$  with propane relative to  $V^+$  by decreasing transition-state energies along the reaction coordinate. In addition, the efficiency of  $H_2$  and  $CH_4$  elimination in the titanium system can be enhanced relative to the

vanadium system because these reactions are spin-allowed from the  $H-M^+-C_3H_7$  intermediate for the former but not the latter metal.

**G. Product Branching Ratios.** To understand the observed  $H_2/CH_4$  branching ratios, consider the reverse reactions  $M^+C_2H_4 + CH_4$  and  $M^+C_3H_6 + H_2$  for both titanium and vanadium systems. In the vanadium system, the initial  $C_3H_6V^+-H_2$  interaction may be substantially greater for triplet  $V^+C_3H_6$  than for quintet  $V^+C_3H_6$  due to the possibility of better back-bonding from the metal ion to the  $H_2$  ligand for triplet  $VC_3H_6^+$ . For example,  $Co^+-H_2$  and  $V^+-H_2$  are bound by 18 kcal/mol<sup>38,39</sup> and 10 kcal/mol,<sup>40</sup> respectively, and the difference is due in large part to the better back-bonding for the  $^3F$ ,  $3d^8$  ground state of  $Co^+$  compared to the  $^3D$ ,  $3d^4$  ground state of  $V^+$ . The binding of triplet and quintet  $V^+C_2H_4$  to  $CH_4$ , however, will be similar because the C-H antibonding orbital of  $CH_4$  is too high in energy for significant back-bonding to occur. As a result, the triplet-quintet splitting for  $C_3H_6V^+-H_2$  (X in Figure 4) may be substantially smaller than for  $C_2H_4V^+-CH_4$  (Y in Figure 4), facilitating  $H_2$  activation in the reverse reaction. This results in a much lower transition-state energy for  $H_2$  elimination than for  $CH_4$  elimination, possibly explaining the dominance of the less exoergic  $H_2$  loss channel.

For  $Ti^+$  reacting with propane, the  $H_2/CH_4$  branching ratio is dominated by  $H_2$  loss even though  $CH_4$  elimination is substantially more exothermic. The reason is again found in the energy of the C-H coupling transition state to eliminate methane relative to the energy of the H-H coupling to eliminate  $H_2$ . In this case, a spin-orbit-coupled crossing is not involved because both  $H_2$  and  $CH_4$  elimination occurs on the doublet surface, increasing the efficiency of both of these reactions relative to those of  $V^+/C_3H_8$ .

## Conclusion

Reactions of first-row transition-metal ions with propane provide substantial insight toward understanding the factors that underlie  $\sigma$ -bond activation. Activation of C-H bonds requires mixing of the ground and excited electronic states of the metal ion to form the molecular orbitals of the inserted intermediates. In the case of the early metals  $Ti^+$  and  $V^+$  reacting with propane, the  $H-M^+-C_3H_7$  intermediate correlates to a component of electronically excited, low-spin,  $3d^n$  states which are 1.12 and 1.45 eV above ground-state  $Ti^+$  and  $V^+$ , respectively. Even so, ground-state  $Ti^+$  ( $^4F$ ) is observed to dehydrogenate and demethanate propane at thermal energy. Ground-state  $V^+$  ( $^5D$ ) is observed to dehydrogenate propane at thermal energy but requires a barrier of 0.7 eV to demethanate propane. These reactions involve spin-orbit-coupled crossings to form doublet  $H-Ti^+-C_3H_7$  and triplet  $H-V^+-C_3H_7$  species.

One difference between the  $Ti^+$  and  $V^+$  systems is that covalent bonding is energetically more favorable for  $Ti^+$  due to facile sd hybridization. This results in greater stabilization of inserted intermediates along the reaction coordinate for  $Ti^+$  and for the products formed:  $D^0(Ti^+-C_3H_6) = 34.5 \pm 3$  kcal/mol and  $D^0(V^+-C_3H_6) = 30.7 \pm 2$  kcal/mol. A further consequence of the stabilization of reaction intermediates and products for  $Ti^+$  is that transition-state energies are reduced and consequently the efficiency for  $Ti^+ +$  propane reactions is

(36) See: *Organometallic Ion Chemistry*; Freiser, B. S., Ed.; Kluwer Academic Publishers: Dordrecht, The Netherlands, 1996; Metal-Ligand Bond Dissociation Energies table.

(37) Hendrickx, M.; Ceulemans, M. Gong, K.; Vanquickenborne, L. J. *Phys. Chem. A* **1997**, *101*, 2465.

(38) Kemper, P. R.; Bushnell, J. E.; vanKoppen, P. A. M.; Bowers, M. T. *J. Phys. Chem.* **1993**, *97*, 1810.

(39) Kemper, P. R.; Bushnell, J. E.; vanHelden, G.; Bowers, M. T. *J. Phys. Chem.* **1993**, *97*, 52.

(40) Bushnell, J. E.; Kemper, P. R.; Bowers, M. T. *J. Phys. Chem.* **1993**, *97*, 11628.



**Table 3.** Input Parameters Used in Phase Space Calculations<sup>a</sup>

|                                   | Ti <sup>+</sup> -C <sub>3</sub> D <sub>2</sub> H <sub>6</sub> <sup>b</sup> | Ti <sup>+</sup> C <sub>3</sub> H <sub>5</sub> D | V <sup>+</sup> -C <sub>3</sub> H <sub>8</sub> <sup>b</sup> | V <sup>+</sup> C <sub>3</sub> H <sub>6</sub> |
|-----------------------------------|----------------------------------------------------------------------------|-------------------------------------------------|------------------------------------------------------------|----------------------------------------------|
| $\Delta_f H_0^\circ$ <sup>c</sup> |                                                                            | 243                                             |                                                            | 256                                          |
| $B^d$                             | 0.20 <sup>e</sup>                                                          | 0.17                                            | 0.20 <sup>e</sup>                                          | 0.17                                         |
| $\sigma^f$                        | 1                                                                          | 1                                               | 1                                                          | 1                                            |
| $\nu_i^g$                         | 2973 <sup>h</sup>                                                          | 3090                                            | 2973 <sup>h</sup>                                          | 3090                                         |
|                                   | 2968(2)                                                                    | 3013                                            | 2968(2)                                                    | 3013                                         |
|                                   | 2967                                                                       | 2991                                            | 2967                                                       | 2991                                         |
|                                   | 2962                                                                       | 2954                                            | 2962                                                       | 2954                                         |
|                                   | 2887(2)                                                                    | 2932                                            | 2887(2)                                                    | 2932                                         |
|                                   | 1476                                                                       | 2871                                            | 1476                                                       | 2871                                         |
|                                   | 1472                                                                       | 1650                                            | 1472                                                       | 1650                                         |
|                                   | 1464                                                                       | 1470                                            | 1464                                                       | 147                                          |
|                                   | 1462                                                                       | 1443                                            | 1462                                                       | 1443                                         |
|                                   | 1451                                                                       | 1420                                            | 1451                                                       | 1420                                         |
|                                   | 1392                                                                       | 1378                                            | 1392                                                       | 1378                                         |
|                                   | 1378                                                                       | 1299                                            | 1378                                                       | 1299                                         |
|                                   | 1338                                                                       | 1171                                            | 1338                                                       | 1171                                         |
|                                   | 1278                                                                       | 1045                                            | 1192                                                       | 991                                          |
|                                   | 1192                                                                       | 991                                             | 1192                                                       | 991                                          |
|                                   | 1158                                                                       | 963                                             | 1158                                                       | 963                                          |
|                                   | 1054                                                                       | 920                                             | 1054                                                       | 920                                          |
|                                   | 940                                                                        | 912                                             | 940                                                        | 912                                          |
|                                   | 922                                                                        | 578                                             | 922                                                        | 578                                          |
|                                   | 869                                                                        | 428                                             | 869                                                        | 428                                          |
|                                   | 748                                                                        | 300                                             | 748                                                        | 300                                          |
|                                   | 369                                                                        | 250                                             | 369                                                        | 250                                          |
|                                   | 268                                                                        | 200                                             | 268                                                        | 200                                          |
|                                   | 250                                                                        | 150                                             | 250                                                        | 150                                          |
|                                   | 216                                                                        |                                                 | 216                                                        |                                              |
|                                   | 200                                                                        |                                                 | 200                                                        |                                              |
|                                   | 150                                                                        |                                                 | 150                                                        |                                              |

<sup>a</sup> Input parameters for H<sub>2</sub>, HD, C<sub>3</sub>H<sub>8</sub>, and CH<sub>3</sub>CD<sub>2</sub>CH<sub>3</sub> have been published (ref 4a). <sup>b</sup> C–H(D) bond activation transition-state complex. <sup>c</sup> Heat of formation at 0 K (kcal/mol). <sup>d</sup> Rotational constant (cm<sup>-1</sup>). <sup>e</sup> Rotational constant assuming the metal ion coordinates with primary hydrogens in the plane of propane. <sup>f</sup> Symmetry number. <sup>g</sup> Vibrational frequencies (cm<sup>-1</sup>) (ref 41). <sup>h</sup> One C–H(D) frequency becomes the reaction coordinate, breaking the C–H(D) bond. Hence, the number of frequencies  $\nu_i = 3N - 7$  where  $N$  is the number of atoms in the molecule.

greater than that for V<sup>+</sup> + propane reactions. In addition, the relative reaction efficiencies might be affected by the fact that Ti<sup>+</sup> reactions require only a single crossing between surfaces of different spin while the formation of ground-state products in the V<sup>+</sup> system requires two such crossings.

Labeling studies were done to probe the nature of the rate-limiting transition states along the reaction coordinate. For ground-state Ti<sup>+</sup> and V<sup>+</sup> reacting with propane, H/D isotope effects on the cross-section data indicate that either a  $\beta$ -H(D) transfer step or a multicenter H<sub>2</sub> elimination step is rate limiting for dehydrogenation. The reductive elimination of methane from a (C<sub>2</sub>H<sub>4</sub>)Ti<sup>+</sup>(H)(CH<sub>3</sub>) intermediate is argued to be rate limiting for demethanation of propane by Ti<sup>+</sup>. The fact that

Ti<sup>+</sup> demethanates propane at thermal energy (where the rate-determining step is spin-conserved) whereas V<sup>+</sup> exhibits a barrier to demethanation suggests the rate-determining transition state for V<sup>+</sup> may occur on the higher energy triplet surface before eventual CH<sub>4</sub> elimination. In this case, a multicenter elimination mechanism cannot be ruled out.

**Acknowledgment.** We gratefully acknowledge the support of the National Science Foundation under Grants CHE94-21176 (M.T.B.) and CHE95-30412 (P.B.A.). Useful conversations with Dr. Jason Perry are also acknowledged.

## Appendix

Statistical phase space theory used to model the experimental KERDs has been previously outlined.<sup>4,5</sup> Three transition states are included in the calculations; two are loose orbiting transition states, one for the reactants and one for the products. The third is a tight transition state due to C–H bond activation,  $\beta$ -H transfer, or H–H coupling. The tight transition state provides competition for the M<sup>+</sup>(C<sub>3</sub>H<sub>8</sub>) adduct to either go on to products or dissociate back to reactants. The probability of the M<sup>+</sup>(C<sub>3</sub>H<sub>8</sub>) complex with energy  $E$  and angular momentum  $J$  going on to products is given by

$$P(E, J) = \frac{F^\ddagger(E, J)}{F_R^{\text{orb}}(E, J) + F^\ddagger(E, J)} \quad (\text{A1})$$

where  $F_R^{\text{orb}}(E, J)$  and  $F^\ddagger(E, J)$  are the microcanonical fluxes through the orbiting transition state back to reactants and through the tight transition state to go on to products, respectively.

Averaging over the energy and angular momentum distribution of the collision complex, the probability for forming products with translational energy  $E_t$  is given by

$$P(E_t) = \frac{\int_0^\infty dE e^{-E/kT} \int_0^{J_{\text{max}}} dJ 2J F_R^{\text{orb}}(E, J) P(E, J) P(E, J; E_t)}{\int_0^\infty dE e^{-E/kT} \int_0^{J_{\text{max}}} dJ 2J F_R^{\text{orb}}(E, J)} \quad (\text{A2})$$

where  $P(E, J; E_t)$  is the fraction of molecules at energy  $E$  and angular momentum  $J$  decaying through the orbiting transition state to yield products with translational energy  $E_t$ . The parameters needed for the calculations are given in Table 3. Rotational constants, polarizabilities, and vibrational frequencies were taken from the literature where possible or estimated from literature values of similar species.<sup>41</sup>

JA974372S

(41) (a) Shimanouchi, T. *Table of Molecular Vibrational Frequencies Consolidated*; National Bureau of Standards: Washington, DC, 1972; Vol. I. (b) Sverdlov, L. M.; Kovner, M. A.; Krainov, E. P. *Vibrational Spectra of Polyatomic Molecules*; Wiley: New York, 1970.